DOI 10.5162/17dss2024/2.3

A new sensor concept to localize non-conducting void fractions in liquid metal based on the measured magnetic field

Lukas Krause[1,2], Nishant Kumar[3], Stefan Gumhold[3], Kerstin Eckert[1,2], Sven Eckert[1], Thomas Wondrak[1]

[1]Institue of Fluid Dynamics, Helmholtz-Zentrum Dresden-Rossendorf, Germany
[2]Institute of Process Engineering and Environmental Technology, TU Dresden, Germany
[3]Institute of Software and Multimedia Technology, TU Dresden, Germany
Kontakt: l.krause@hzdr.de

Introduction

Electrolytically produced hydrogen using renewable energy is a key energy carrier in transitioning to green energy. Hydrogen and oxygen as the desired products are evolving in form of gas bubbles during water electrolysis upon application of a current. However, the gas bubbles are not electrically conductive, block electrocatalytically active surface on the electrodes during their growth and thus reduce the overall efficiency [1]. Measurement techniques such as X-ray tomography can localize the gas bubbles [2], but the process to implement them in industrial electrolyzers is complex. Information about the distribution of electrical conductivity σ can be derived from the magnetic field generated outside the electrolyzer by the current inside the cell. Gradients of σ, such as those between electrolyte solution and gas bubbles, modify the distribution of the electric current density $\boldsymbol{j}$, whose structure determine the shape of the magnetic flux density $\boldsymbol{B}$.

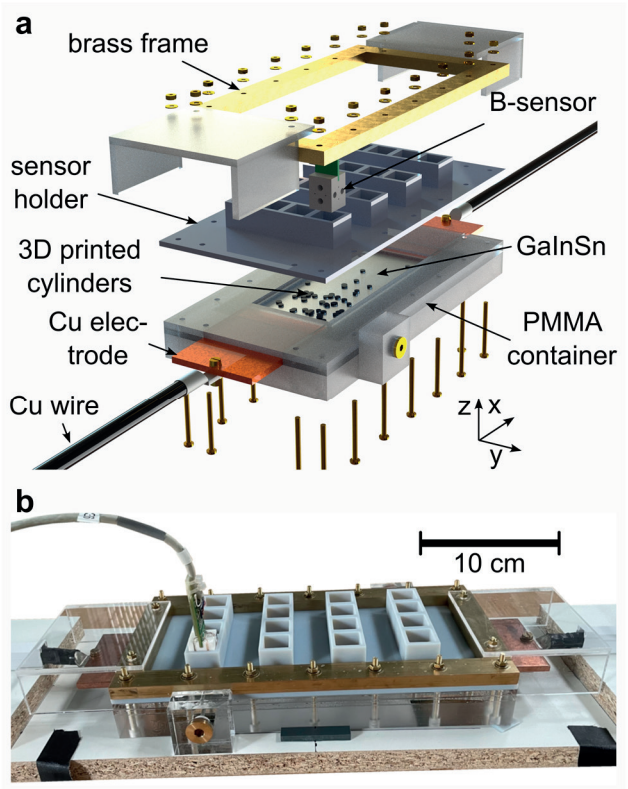

Fig. 1: (**a**) Explosion view and (**b**) photo of the assembled experimental setup.

This study proposes a new method that is easily installable, non-intrusive and reconstructs the conductivity distribution within the cell based on $\boldsymbol{B}$ measurements, thus enabling the localization of non-conductive fractions.

Materials and Methods

Setup

Within this work, the possibility of reconstructing the electrical conductivity from the measurable magnetic flux density is studied numerically and experimentally in a Proof-of-concept model (POC).
The water electrolyzer in the POC model is simplified by an electrical conductor with significant differences in electrical conductivity, shown in Figure 1. Electrodes of Cu contact the electrochemically non-reactive and resting liquid metal $Ga_{67}In_{20.5}Sn_{12.5}$ (in wt%, *GaInSn*) with a current density of 1 A/cm^2 which is in the range of industrially applied current densities in water electrolysis. An almost 2-dimensional channel (length × width × height = 16 × 7 × 0.5 cm^3) is filled with conductive *GaInSn* (σ_{GaInSn} = 3.3 MS/m) and electrically insulating cylinders, representing the gas bubbles. An array of magnetic flux density sensors is positioned above the volume of *GaInSn*. During the experiments, a FluxGate sensor (FOERSTER, Reutlingen, Germany) was used for measuring $\boldsymbol{B}$. Given the sensor's spatial dimensions and assuming the possibility of a simultaneous measurement at each of the positions, only 4 × 4 detectors can be placed in the x-y-plane (cf. coordinate system in Figure 1a). Since water electrolysers obtain components as e.g. sealing and screwing of the cell stack, a certain spacing is requiered between measurement positions and the current-conducting part of the cell. Therefore, the sensor plane is located in 25 mm distance to the current-carrying plane during the experiments. The detector positions are equally spaced along the x- and y-axis within a plane. In addition, the $\boldsymbol{B}$ fields are simulated at 50 × 50, 10 × 10 and 4 × 4 positions in 3 mm and 25 mm distance to to conductor.

Simulation, Reconstruction and Experiment

After simulating the electric current density

$$\boldsymbol{j}(\boldsymbol{r}') = -\sigma(\boldsymbol{r}')\nabla\big(\varphi(\boldsymbol{r}')\big)$$

from a given electrical conductivity σ and the negative gradient of the scalar electric potential φ at a position $\boldsymbol{r'}$ in 3D space inside the conductor, the magnetic flux density

$$\boldsymbol{B}(\boldsymbol{r}) = \frac{\mu_0}{4\pi}\iiint_V \frac{\boldsymbol{j}(\boldsymbol{r}') \times (\boldsymbol{r} - \boldsymbol{r}')}{|\boldsymbol{r} - \boldsymbol{r}'|^3} dV'$$

at a three-dimensional position outside the conductor $\boldsymbol{r}$ can be calculated by solving Biot-Savart's law with using the magnetic permeability of the vacuum μ_0 of $4\pi \cdot 10^7$ N/A^2 and incorporating the volume element dV' of the current density $\boldsymbol{j(r')}$.

By simulating $\boldsymbol{B(r)}$ and $\boldsymbol{j(r')}$ from $\sigma(\boldsymbol{r'})$, utilizing the finite element software COMSOL Multiphysics 6.0, a data set of various geometrical configurations of the POC model was generated and used for training of an invertible neural network (INN). The INN is employed for reconstructing $\sigma(\boldsymbol{r'})$, based on the magnetic flux density at 4 × 4 sensors in 25 mm distance to the conductor. Solely, the x-component of the $\boldsymbol{B}$ field was chosen to be fed into the INN, as sensors in future experiments are possibly not able to detect all three vector components and $\boldsymbol{B}_x(\boldsymbol{r})$ contains the most information about the location of non-conductive void fractions. Within the dataset, the spatial distributions, numbers and sizes of the non-conductive cylinders (d_{cyl} = 4…5 mm) are varied. The resolution of the initially unstructured tetrahedral mesh, that was used for the simulation of $\boldsymbol{j(r')}$ from $\sigma(\boldsymbol{r'})$, was reduced by interpolating on a structured mesh of hexahedrons. The structured grid obtains a fixed number of mesh cells, needed as constant input dimension for the INN training. Simulation, INN and reconstruction are explained in detail in Kumar et. al [3].

In addition to the training data set, one additional configuration of bubble distributions was simulated and physically replicated. Instead of utilizing 16 detectors in the 4 × 4 array, only a single sensor was used for all positions, which allows a more targeted focus on the elimination of measurement errors. Since the amplitude of the $\boldsymbol{B}_x(\boldsymbol{r})$ is rather small compared to $\boldsymbol{B}_y(\boldsymbol{r})$ and $\boldsymbol{B}_z(\boldsymbol{r})$ in the POC model, slight tilting of the sensor results significant deviations around the unbiased $\boldsymbol{B}_x(\boldsymbol{r})$ through the partially detected y- and z-components. In order to minimize disturbing electromagnetic fields, ferromagnetic parts were removed in the vicinity of the setup. The FluxGate sensor was placed in a 3D printed holder (DraftGrey, Objet30 Prime V5) which was fixed through a brass frame and brass screws to the *PMMA* channel that contains *GaInSn*, as shown in Figure 1. Replicating the void fractions of the simulation, electrically non-conducting, 3D printed cylinders were inserted into the liquid metal. Due to the high surface tension of *GaInSn*, the cylinders were carefully brushed with the liquid metal before filling the channel to guarantee their complete wetting.

Results

A data set comprising σ, $\boldsymbol{j}$ and $\boldsymbol{B}$ distributions of 10,000 geometric configurations of different cylinder distributions was generated numerically to train an INN for the reconstruction of $\sigma(\boldsymbol{r'})$. Additionally, one configuration of the POC model that is not contained in the training data set was simulated, physically replicated and in the following used exemplarily for visualizations.

Figure 2a shows $\sigma_{rel}(\boldsymbol{r'})$, normalized by the conductivity of *GaInSn*, at the central plane inside the conductor where non-conducting areas are marked in blue. Below, the resulting absolute current density is displayed, implying the presence of the cylinders by local extrema in their vicinity. Calculated from $\boldsymbol{j(r')}$, the coarsely resolved $\boldsymbol{B}_x(\boldsymbol{r})$ of the 4 × 4 sensor array in 25 mm distance to the conductor is shown in Figure 2c.

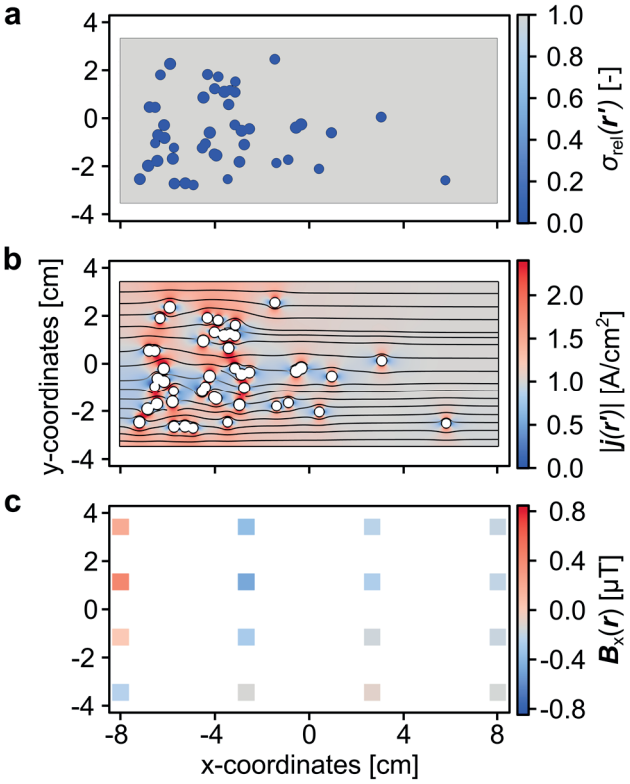

Fig. 2: Numerical results of (**a**) $\sigma_{rel}(\boldsymbol{r'})$ and (**b**) $|\boldsymbol{j(r')}|$ at the central plane inside the conductor and (**c**) $\boldsymbol{B}_x(\boldsymbol{r})$ of 4 × 4 sensors at 25 mm distance to the conductor.

The amount of detectable local details of the magnetic flux density depends on the number of employed sensors and their distance to the conductor. Figure 3 shows numerically generated $\boldsymbol{B}_x(\boldsymbol{r})$ for 50 × 50, 10 × 10 and 4 × 4 sensors in 3 mm and 25 mm distance to to conductor. Close to the *GaInSn* containing volume (Figure 3a to 3c), the $\boldsymbol{B}$ field contains numerous local features. The amount of local extrema is decreasing upon reducing the number of detectors until the unsuffiecient resolution of 4 × 4 sensors is incapable of resolving them. When measuring further away at a distance of 25 mm to the

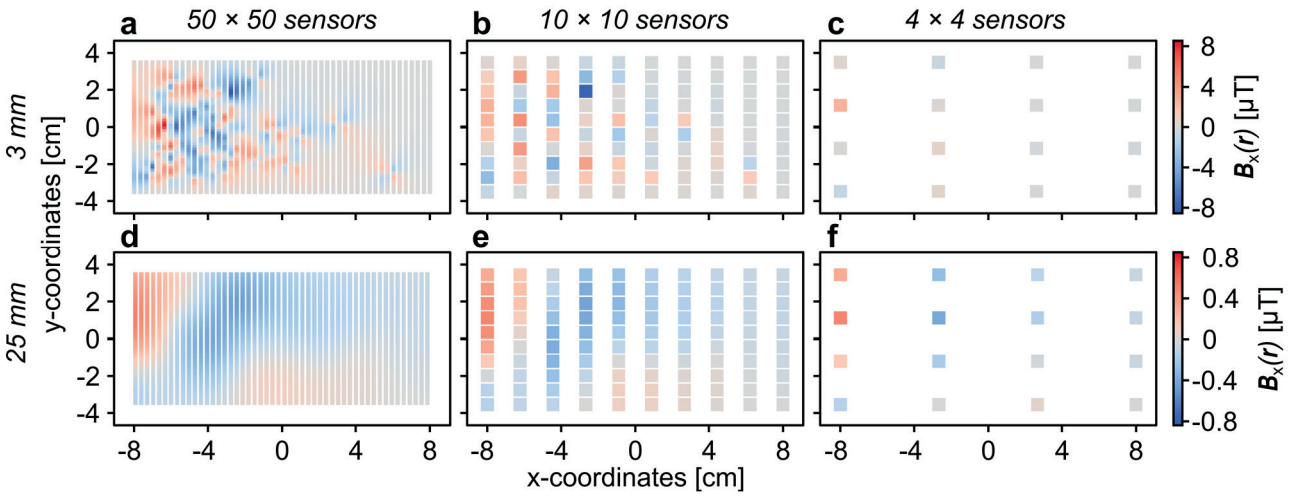

Fig. 3: B_x at 50 × 50, 10 × 10 and 4 × 4 sensors, calculated at a distance of 3 mm (**a** to **c**) and 25 mm (**d** to **f**) from the conductor.

conductor (Figure 3d to 3f), the amount of local features decreases even for the 50 × 50 array and only a blurry generalized B_x distribution can be be detected. The signal's amplitude decreases about one order of magnitude compared to the 3 mm case. Only 4 × 4 sensor values at 25 mm distance are used as INN input. The aforementioned constraints and the utilization of solely one vector component of B posing a challenge for the reconstruction, wherefore smaller sensors are desirable for future experiments.

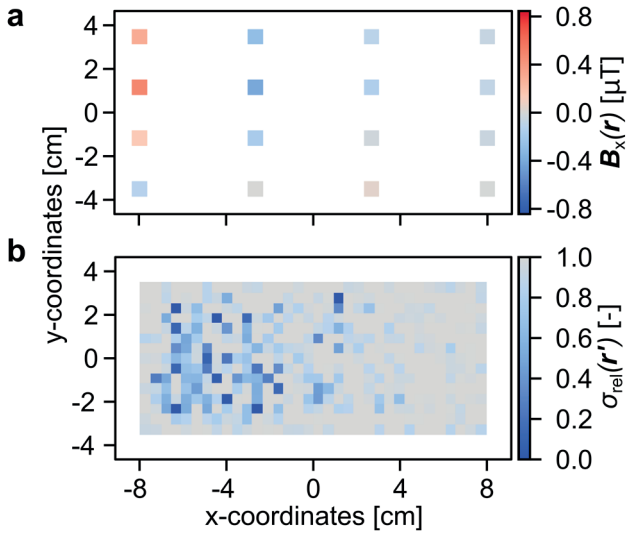

Fig. 4: (**a**) Experimentally measured B_x distribution at a distance of 25 mm from the conductor and (**b**) INN reconstruction of $\sigma_{rel}(r')$ derived from the measured $B_x(r)$.

Figure 4a shows the experimentally measured B_x field which is in good agreement to the simulated results, as depicted in Figure 3f. The deviations of 9.6 nT on average can be explained by unavoidable minor tiltings of the senor, the not entirely simulated wiring of the experimental setup to the power supply and cylinders possibly incompletely wetted with *GaInSn*. Based on that B field, the trained INN is capable of reconstructing $\sigma_{rel}(r')$ in real-time, displayed in Figure 4b with the aforementioned coarser resolved mesh that was needed for confining the INN training data's dimensions. Although the reconstruction exhibit noise, when comparing to the conductivity distribution in Figure 2a, larger agglomerations of non-conductivities are recognizable and can be localized.

Conclusion

This proof-of-concept study successfully demonstrated the localization of agglomerations of electrically non-conductive fractions in a conductive liquid by reconstructing the electrical conductivity distribution based on the non-intrusively measured B_x field. For the real-time reconstruction, an INN was used that had been trained with a vast, numerically generated data set. Not included in the training data set, an additional configuration of the POC model was simulated and physically replicated. Therein experimentally measured B_x distributions were used as INN input. Since the sensor array can be installed also at already existing setups, future research could focus on employing the sensor concept to real water electrolysis cells as a viable bubble detecting technique.

References

[1] Zhao, X.; Ren, H.; Luo, L. Gas Bubbles in Electrochemical Gas Evolution Reactions. *Langmuir* **2019**, 35 (16), 5392–5408.

[2] Lee, Ch.; Lee, J. K.; Zhao, B.; Fahy, K. F.; Bazylak, A. Transient Gas Distribution in Porous Transport Layers of Polymer Electrolyte Membrane Electrolyzers. *J. Electrochem. Soc.* **2020**, 167 (2), 024508.

[3] Kumar, N.; Krause, L.; Wondrak, T.; Eckert, S.; Eckert, K.; Gumhold, S. Robust Reconstruction of the Void Fraction from Noisy Magnetic Flux Density Using Invertible Neural Networks. *Sensors* **2024**, 24 (4), 1213.

Acknowledgements

This work was financially supported by the School of Engineering of TU Dresden in the frame of the Hydrogen Lab and the German Helmholtz Association in the frame of the project “Securing raw materials supply through flexible and sustainable closure of material cycles”. It was also supported by the Center for Scalable Data Analytics and Artificial Intelligence (ScaDS.AI) Dresden/Leipzig, Germany, and was also partially funded by the Federal Ministry of Education and Research of Germany in the joint project 6G-life (16KISK002) and by DFG as part of the Cluster of Excellence CeTI (EXC2050/1, grant 390696704). The authors gratefully acknowledge the Center for Information Services and HPC (ZIH) at TU Dresden for providing computing resources.